Performance Evaluation of Interior Permanent Magnet Synchronous Machines using Deadbeat-Direct Torque Flux Control in an Indirect Matrix Converter with a Reactor Free Boost Converter

Goh Teck Chiang Jun-ichi Itoh
Nagaoka University of Technology
Nagaoka Niigata, 940-2188, Japan
tcgoh@stn.nagaokaut.ac.jp itoh@vos.nagaokaut.ac.jp

Jae Suk Lee Robert D. Lorenz
University of Wisconsin-Madison, WEMPEC
Madison, WI 53706 USA
lee82@wisc.edu r.d.lorenz@ieee.org

***Abstract* – This paper discusses the performance of an interior permanent magnet synchronous machine by using deadbeat-direct torque flux control (DB-DTFC) in a hybrid power circuit structure, which consists of an indirect matrix converter (IMC) and a reactor free boost converter (RFBC). The first section of this paper documents the performance of DB-DTFC when carrier comparison PWM and space vector modulation (SVM) are used as modulation techniques. Corresponding Volt-sec solutions for each modulation technique are shown via simulation and experiments. The second section discusses DB-DTFC properties in the proposed IMC/RFBC circuit. The results demonstrate that DB-DTFC is capable of delivering fast dynamic torque response in one sample period even when (i) variable switching frequency is applied in the inverter of the IMC and (ii) DC offset current occurs in the output current of the IMC.**

***Index Terms*— Indirect Matrix Converter, PWM, AC/AC converter, Over modulation, Square wave, Trapezoidal wave**

I. INTRODUCTION

Energy saving converters driving high speed synchronous motors have been studied extensively for transportation applications such as the hybrid electric vehicle (HEV). The classical circuit structure, which is composed of a back-to-back (BTB) converter and a boost converter (BC), is typically applied in such applications [1, 2]. However, the classical circuit faces size and thermal challenges. First of all, the classical circuit requires numbers of film capacitors in the DC bus for the control. These passive components, capacitors and boost reactors, are heavy and bulky. Therefore, size reduction of converters for automotive application is challenging. Furthermore, temperature control is another serious issue for transportation applications. As these passive components disallow to operate under a high temperature environment, cooling system becomes essentially important. Including the cooling system for these passive components, the size of the entire system becomes even larger.

One of AC/DC/AC converter topologies actively considered for HEV applications is the indirect matrix converter (IMC) [3, 4]. The IMC can be manufactured in small size because electrolytic capacitors are not required to maintain a DC link voltage. In [5, 6], a circuit structure was proposed in which an IMC is connected to a boost converter with batteries connected to the neutral point of a motor, effectively creating a reactor free boost converter (RFBC). In the proposed IMC/RFBC circuit structure, two passive components, DC link electrolytic capacitors and separate boost reactors, were removed while reducing the size and weight of the system, yet achieving high efficiency (up to 94% was demonstrated [5, 6]).

However, for the HEV application, a robust motor control technique is required to deliver torque over a wide range of controlled speed. The proposed IMC/RFBC circuit has not been integrated with a regularly sampled direct torque control (DTC) that directly controls both flux linkage and torque [7, 8]. It should be noted that the proposed IMC/RFBC circuit structure uses variable switching frequency to achieve zero current switching (ZCS) with a corresponding reduction in switching losses. Variable switching frequency is not directly compatible with DTC configured for regular sampling in which PI controllers are used to control both flux and torque. Furthermore, adapting to load torque and speed changes and to parameter variations is slow because regularly sampled DTC that uses PI controllers does not deal with the cross-coupling between torque and flux linkage.

This paper clarifies the performance of an interior permanent magnet synchronous machine (IPMSM) by using a robust motor control technique known as Deadbeat-direct torque and flux control (DB-DTFC) in the proposed IMC/RFBC circuit. DB-DTFC is a regularly sampled alternative to PI-DTC that is capable of achieving fast dynamic torque response [9, 10]. Furthermore, torque and flux linkage are directly controlled via DB-DTFC in a fully decoupled manner. In the proposed IMC/RFBC circuit, due to the RFBC connection, DC offset occurring in the output current depending on the polarity and value of the battery current. Since the torque is subjected to the motor current in general, this phenomenon is required to study and analyze as a part to confirm the proposed IMC/RFBC circuit is capable to operate with DB-DTFC to produce a fast torque response.

The first section of this paper evaluates the performance of DB-DTFC when using the Volt-sec vectors produced by two standard PWM schemes, namely space vector modulation (SVM) and carrier comparison PWM, in an inverter. Sufficient results are provided to distinguish the maximum Volt-sec and torque ripple that are produced by the two modulation schemes. The second section discusses the performance of the DB-DTFC in the proposed IMC/RFBC circuit structure. The performance of a standard inverter is discussed in first section because the secondary stage of the IMC is similar to an inverter; however, in IMC the control of the inverter will be implemented with variable switching frequency. In addition, the proposed circuit structure has known properties that must be dealt with, i.e. DC offset

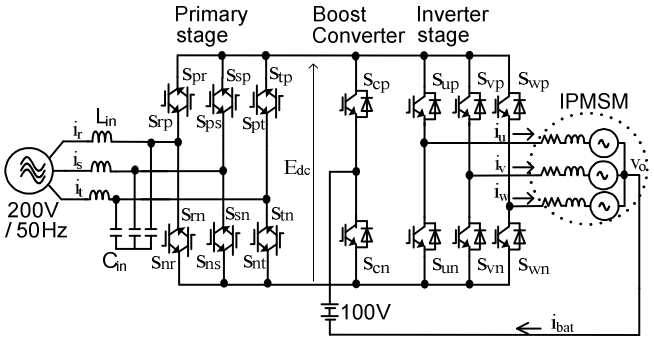

Fig. 1 Proposed circuit structure.

current occurring in the output current due to the neutral point connection. These phenomenons are discussed and evaluated in the last section to document that the proposed circuit structure is capable of delivering fast dynamic torque response with DB-DTFC.

II. CIRCUIT TOPOLOGY

Fig. 1 shows the proposed IMC/RFBC circuit configuration based on an indirect matrix converter [3, 4]. The indirect matrix converter can be divided into primary stage and secondary stage. The primary stage for the 3-phase input power source consists of twelve IGBT devices, which is also known as a current source rectifier. It can be replaced with RB-IGBT to achieve higher efficiency. The structure is direct AC-to-AC conversion and it does not require electrolytic/ film capacitors to control the DC link voltage. An LC filter is used at the primary side to smooth the input current during the switching intervals. The secondary stage consists of six IGBTs in a standard voltage source inverter configuration that is connected to a motor. Moreover, a boost converter and batteries, which are used as the secondary input power source, are connected at the DC bus. The boost converter is connected to the neutral point of the motor and utilizes the leakage inductance of the motor for its operation; thus acting as a RFBC. The proposed circuit achieves a compact hybrid power system that can deliver high energy conversion efficiency.

III. DEADBEAT-DIRECT TORQUE & FLUX CONTROL

Since DB-DTFC is developed via a model inverse solution, the DB-DTFC calculates the Volt-sec vector solution needed to produce the desired torque and flux by the end of each switching (sample) period. Moreover, inverters source with "Volt-seconds", DB-DTFC operates with one control law over the entire operating space.

The IPMSM torque equation is shown in (1). The differential torque equation can be written in discrete time as (2) [10], where T_S is the switching period (sampling time), P is the number of poles, v_d is the d-axis voltage, v_q is the q-axis voltage, L_d is the d-axis inductance, L_q is the q-axis inductance, λ_d is the d-axis flux linkage, λ_q is the q-axis flux linkage, λ_{pm} is the permanent magnet flux linkage, R_S is the stator resistance, and ω_r is the angular velocity.

$$T_{em} = \frac{3}{4} P\left[\lambda_{pm} i_q - (L_q - L_d) i_q i_d\right] \tag{1}$$

$$\begin{aligned}\frac{T_{em}(k+1)-T_{em}(k)}{T_s} &= \frac{3}{4}P\left[v_d(k)\lambda_q(k)\left(\frac{L_d-L_q}{L_dL_q}\right)+v_q(k)\frac{(L_d-L_q)\lambda_q(k)+\lambda_{pm}L_q}{L_dL_q}\right.\\ &+\frac{\omega_r(k)}{L_dL_q}((L_q-L_d)(\lambda_d^2(k^2)-\lambda_q^2(k^2))-L_q\lambda_d(k)\lambda_{pm})\\ &\left.+\frac{R_s\lambda_q(k)}{L_d^2L_q^2}((L_q^2-L_d^2)\lambda_d(k)-L_q^2\lambda_{pm}\right]\end{aligned} \tag{2}$$

Also, the IPMSM state equation is expressed in terms of complex vector form of stator flux linkage (λ_{dq}) in discrete time in the rotor frame as (3).

$$\begin{aligned}\lambda_{dqs}(k+1) &= \lambda_{dqs}(k) + v_{dqs}(k)T_s\\ &-\left(\frac{R_s}{L_s}+j\omega_r\right)\lambda_{dqs}(k)T_s+\frac{R_s}{L_s}\lambda_{pm}T_s\end{aligned} \tag{3}$$

By substituting (3) into (2), (2) becomes a function of torque and stator voltage. This relationship can be rewritten as (4) to show the linear relationship of d and q-axis voltage with slope, including the command changes in torque [10].

$$v_q(k)T_s = Mv_d(k)T_s + B \tag{4}$$

where,

$$M = \left(\frac{(L_q-L_d)\lambda_q(k)}{(L_d-L_q)\lambda_d(k)+L_q\lambda_{pm}}\right)$$

$$\begin{aligned}B = \left(\frac{L_dL_q}{(L_d-L_q)\lambda_q(k)+\lambda_{pm}L_q}\right)\left[\frac{4\Delta T_{em}}{3}-\frac{\omega_r T_s}{L_dL_q}((L_q-L_d)\right.\\ (\lambda_d^2(k^2)-\lambda_q^2(k^2))-L_q\lambda_d(k)\lambda_{pm})\\ \left.-\frac{R_sT_s\lambda_q(k)}{L_d^2L_q^2}((L_q^2-L_d^2)\lambda_d(k)-L_q^2\lambda_{pm}\right]\end{aligned}$$

The deadbeat controller block shown in Fig. 2 represents (4), where the v_{dq} voltage vector is calculated. These signals are forwarded into the IMC controller to obtain the desired

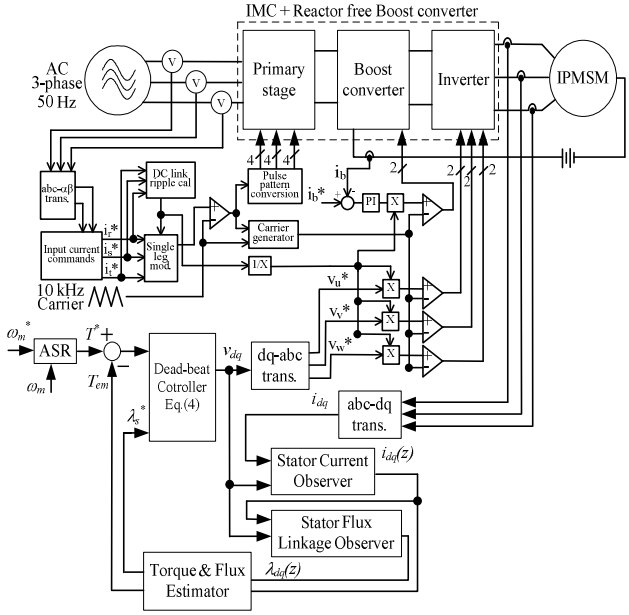

Fig. 2 DB-DTFC control diagram for the proposed circuit.

switching pulses for inverter by using variable switching frequency carrier comparison PWM (for the case of inverter, the front end is connected with a standard full bridge rectifier, the controller is a 10 kHz carrier comparison PWM or a space vector modulation (SVM)). The control details for the proposed IMC/RFBC structure has been discussed in [3, 4]. Furthermore, since the flux linkage cannot be measured, a stator flux linkage observer based on a voltage model and a current model is included to estimate the flux in time domain. In addition, a stator current observer is included in order to reduce the sampling delay and improve the estimation for the flux linkage. The stator current at the next sample instants is estimated in the discrete time via the stator current observer [9, 10].

IV. Performance Comparison of an Inverter between Carrier Comparison PWM and SVM

In DB-DTFC using a fixed switching frequency, the use of stator flux linkage as a control variable allows the construction of a graphical representation of the Volt-sec vector solution that achieves the commanded torque and stator flux magnitude in one sample period. This section discusses the difference and maximum of Volt-sec that can be achieved by applying either space vector modulation (SVM) and carrier comparison PWM to produce the desired Volt-sec. vector. Second, the torque line from the two modulations are compared and analyzed experimentally. Note that the controller is similar to Fig. 2. However, for this work, the inverter is disconnected from the IMC/RFBC and directly connected with a full bridge rectifier. Then, the inverter controller is changed into the standard carrier comparison PWM (10 kHz switching frequency) and SVM, for evaluation of each modulation scheme. The motor parameters used for simulation are shown in Table 1.

Table 1. Simulation/Experiment and motor parameters

DC link voltage	300 V	Switching frequency	10 kHz
Motor rated speed	1280 RPM	Stator resistance	1.5 ohm
d-axis inductance	8 mH	q-axis inductance	22 mH
Poles	4	Rated torque	2.26 N.m
Inertia	0.0016	Flux induced	0.12

A. Simulation results for DB-DTFC modulation schemes

The simulation results of the inverter from each modulation scheme are shown in Fig 3, where 3(a) is the carrier comparison PWM and 3(b) is the SVM. The motor speed is controlled by the load to be 1000 RPM and a step signal is provided as the torque command.

For the simulation, stator flux linkage that minimizes copper losses is used at given torque commands. Both the results demonstrate that the estimated torque lines can respond very fast to the torque commands, regardless of the modulation schemes. Besides, the estimated flux is also shown closely tracking with the flux command, as the torque command has changed.

B. Volt-sec utilization for DB-DTFC modulation schemes

Fig. 4 shows the graphical solution of Volt-sec between the two modulation schemes. The motor speed is 500 RPM and the torque command is controlled as a step transient from 0 Nm to 2 Nm. It takes several time steps to achieve the commanded torque due to insufficient amount of voltage. The total sample time required to achieve the torque is obtained, which is the total steps that the voltage magnitude ($Vdqs$) requires to produce and reach the desired torque. Each time step also represents the maximum voltage

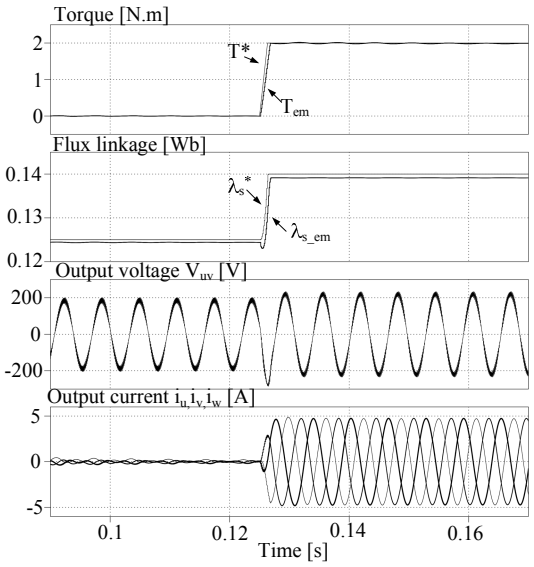

(a) Carrier comparison PWM

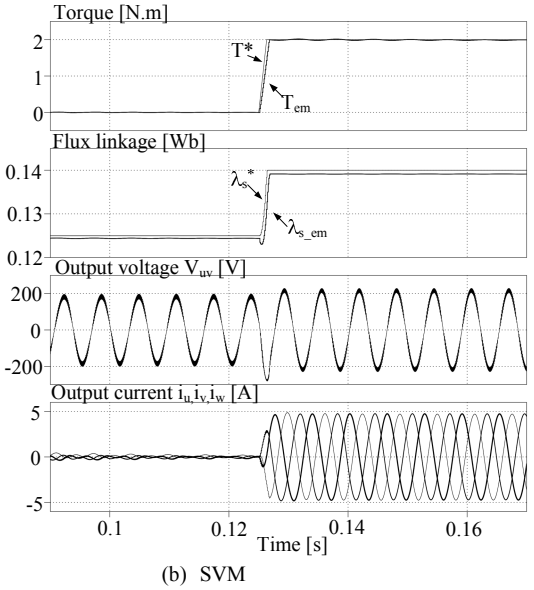

(b) SVM

Fig. 3 Simulation results for the two modulation schemes for a torque step transient and the motor speed constant at 1000 RPM.

magnitude can be produced by the modulation. In this case, the average voltage magnitude is 139 V for SVM and 137 V for carrier comparison PWM. The voltage utilization of the SVM is 1.5% higher than that of the carrier comparison PWM. Even though the carrier comparison produces a lower voltage magnitude, the total time steps required to change the torque is not significantly different from SVM.

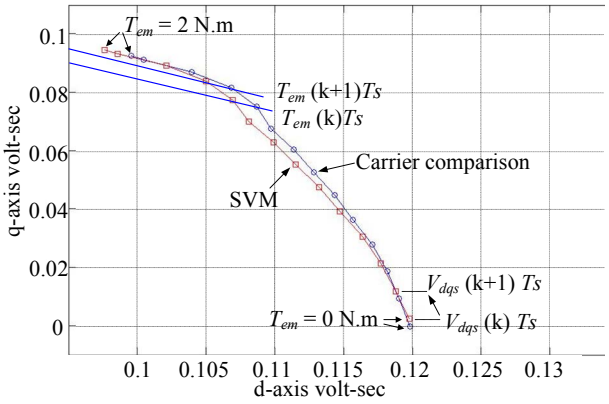

Fig. 4 Graphical Volt-sec. solution for the two modulation schemes

C. *Experimental results for DB-DTFC modulation schemes*

Fig. 5 shows the torque responses, to a ramp torque command, obtained by from the two inverter modulation schemes, SVM and carrier comparison PWM. The motor speed is 300 rad/sec in Fig. 5(a) and 550 rad/sec in Fig. 5(b), respectively. Note that in the experiments, the carrier comparison PWM includes third harmonic injection. Under the medium speed condtions as shown in Fig. 5(a), no signficant difference can be noticed between the two modulations. Both estimated torque lines can achieve the command value. For Fig. 5(b), the speed is increased to 550 rad/sec, and carrier comparison PWM is able to obtain the torque close to the desired value because a higher voltage magnitude can be produced.

V. Performance Evaluation of the Proposed IMC/RFBC Circuit Structure

This section discusses the performance of the proposed IMC/RFBC circuit structure with the implementation of DB-DTFC. The proposed circuit has several properties that need to be addressed. First, in order to reduce the switching losses, frequent zero vectors are required in the inverter stage of the IMC. This is because the zero vector periods cause the output current to circulate within the inverter and the DC link current becomes zero, which will enable ZCS on all the switching devices in the primary stage of IMC. In order to enable ZCS, an unique carrier that has variable switching frequency is formed and applied to the inverter stage of IMC.

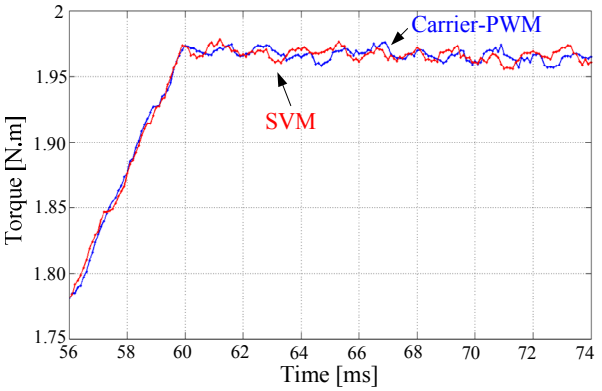

(a) Comparison of torque ripple when motor speed is 300 rad/sec.

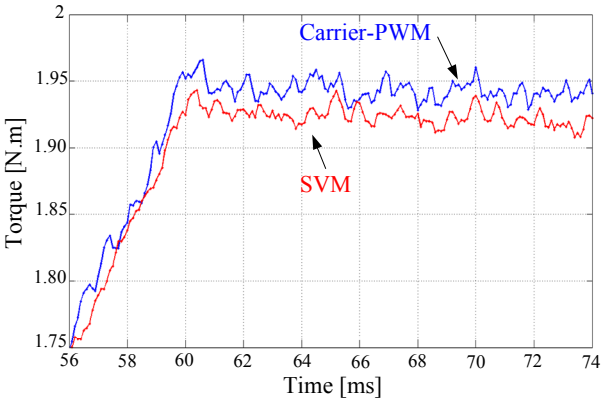

(b) Comparison of torque ripple when motor speed is 550 rad/sec.

Fig. 5. Comparison of torque ripple between carrier-PWM and SVM at different operating conditions (a) 300 rad/sec (b) 550 rad/sec

However, variable switching frequency is not favorable in a traditional inverter as the torque ripple will become higher, which will increase motor losses [11].

On the other hand, the RFBC that connects to the neutral point of a motor is a dependent circuit requires the inverter to operate successfully.

Due to this dependency relationship, the battery current is added into the inverter current. As a result, the motor current consists of battery current that will cause a DC offset.

In this section, the fundamental operation of proposed circuit with the implementation of DB-DTFC is verified in simulation using the motor parameters shown in Table 1. Then, torque response and ripple are analyzed experimentally with the IPM motor specified in Table 2.

Table 2. Experimental conditions and motor parameters

Input voltage	200 V	Input frequency	50 Hz
Battery voltage	50 V	Switching frequency	10 kHz
Motor rated voltage	180 V	Motor rated current	6.1 A
Motor rated speed	1800 RPM	Number of Poles	6

Stator resistance	1.56 ohm	d-axis inductance	11.5 mH
Flux induced	0.308	q-axis inductance	23 mH
Inertia	0.00255		

A. Voltage Utilization for the DB-DTFC IMC

Similar to the previous fixed switching frequency modulation comparison for the inverter, the voltage utilization of IMC for the variable frequency carrier comparison PWM is discussed here. Fig. 6 shows the graphical Volt-sec. solution for the IMC variable frequency carrier comparison PWM and inverter SVM. Note that in this case, the value of DC voltage of the inverter is similar to the DC link voltage of the IMC. The motor speed is 900 RPM and the torque is controlled as a step transient from 0 Nm to 2 Nm. In this case, the average voltage magnitude produced by SVM and IMC variable frequency PWM is 145 V and 143 V respectively. Note that, even though the IMC produces more switching counts per sample period (T_S), the average voltage magnitude in time domain is nearly the same as the standard carrier comparison PWM, which is 1.5 % less than the SVM.

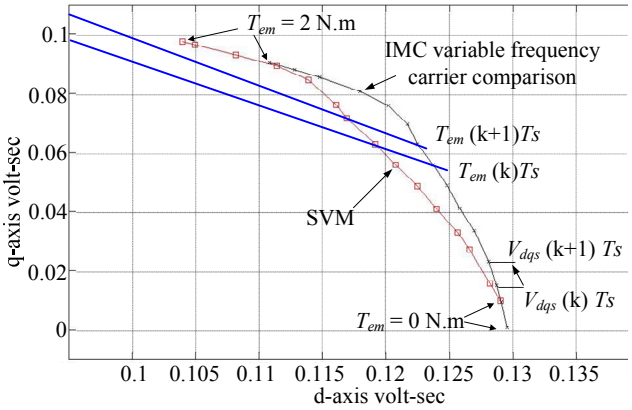

Fig. 6 Graphical Volt-sec. solution for the IMC variable frequency carrier comparison PWM and inverter SVM showing the voltage utilization of the SVM is 1.5% higher than that of the IMC carrier comparison PWM.

B. Simulation Results for the DB-DTFC IMC/RFBC

Fig. 7 demonstrates the effectiveness of the DB-DTFC in the proposed circuit. The motor parameter is similar to Table 1, the input voltage is 200 V, the input frequency is 50 Hz, the battery voltage is 100 V and the switching frequency is 10 kHz.

Closed loop velocity control (ASR as shown in Fig. 2) is used to accelerate and decelerate the motor. Feasible control over the two input power sources (generator and battery) is also demonstrated in the results. The acceleration starts at 0.1s, it can be noticed that the estimated torque rises as a step transient immediately. Also, the input power for the entire acceleration range is controlled by the battery power. Notice that the input current remains constant and then the battery power increases gradually during the acceleration; as so, the DC offset in the output current becomes significantly noticeable as the battery current becomes larger.

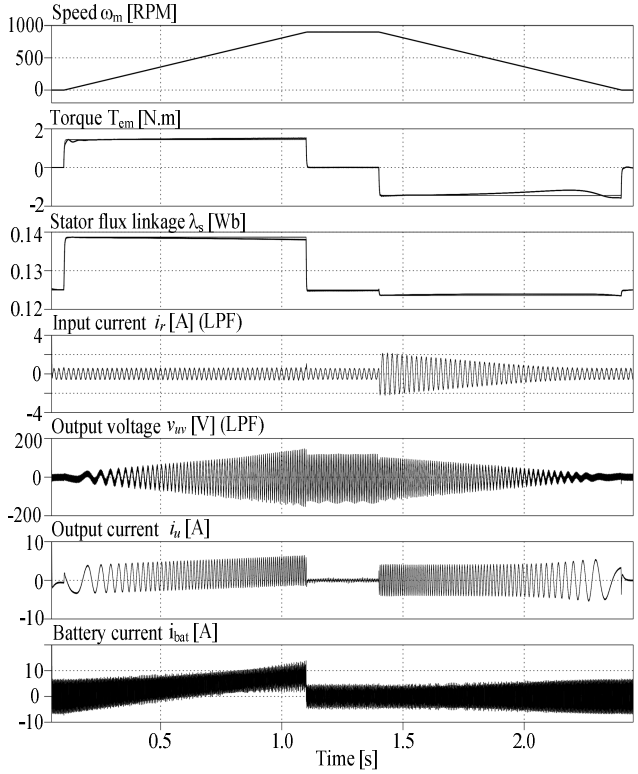

Fig. 7 Control of acceleration and deceleration with DB-DTFC showing that the battery power is used during acceleration and the generator power is used during deceleration.

The DB-DTFC acceleration results demonstrate that despite the utilization of battery current, which causes an offset in output current, the drive produces an estimated torque closely matching the commanded torque.

At time 1.1s, the motor speed achieves the desired speed value and the torque is nearly zero. The motor speed remains at the same speed for 0.3s. Deceleration starts at 1.4s, the input power for the entire deceleration range is powered by generator power (input source). A negative torque is produced that closely matches the torque command, similar to the case of acceleration, until the speed reaches to zero at 2.5s. This result shows that the hybrid power management from two input sources can enable the DB-DTFC to produce the torque commanded by the velocity loop.

Fig. 8 shows the input and output signals of the *idq* components in the stator current observer, under the same conditions as Fig. 7. The input signals consist of a high amount of ripple because the battery current is included in the output current. From the results, it shows that the DC offset caused by battery current does not affect the dq-axis components of the output current. Moreover, the stator current observer is able to filter out the ripple and estimate the next sample signal accurately. The results also show that

the output signals track the input signals as the torque command changes.

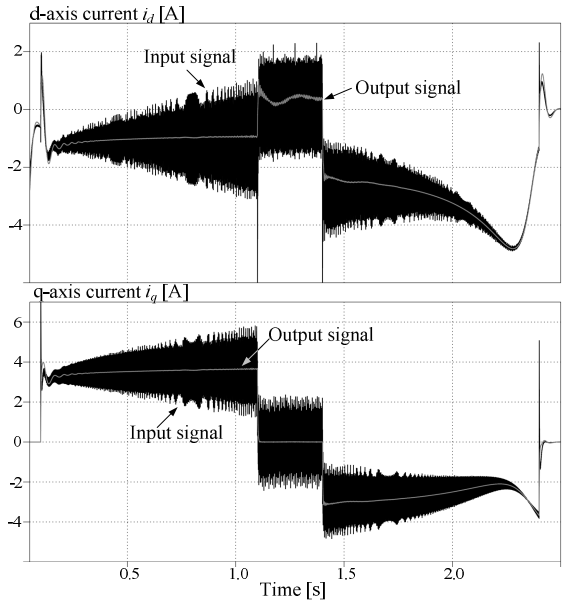

Fig. 8 Input and output signals for the i_{dq} components in the stator current observer.

C. *Experimental Results for the DB-DTFC IMC/RFBC*

Table 2 shows the experiment condition and motor parameters that have tested in the proposed circuit structure. Note that velocity control is not used in the following results in order to analyze the true torque response. Initially, the load machine runs at low speed nearly at 100 RPM. The proposed circuit/motor is then driven by the speed of the load machine during the start-up.

Fig. 9 shows the experimental results obtained from the IMC only, i.e. the RFBC is disconnected from the IMC. A torque step command from 0 Nm to 5 Nm is applied. Torque ripple occurs at nearly 0 Nm due to the "cogging torque". From the results, the estimated torque very closely tracks the torque command. Furthermore, the torque response is extremely fast to reach 5 Nm.

Fig. 10 shows the experimental result which is obtained from DB-DTFC using the proposed IMC/RFBC circuit. In this result, the battery power is used instead of input current when the output current is responding to the torque. Comparing to the result in Fig. 9, the input current remains unchanged, indicating that battery current is utilized as the input power source. However, due to the absence of any active power management for the two input sources (grid and battery), part of the battery energy goes into the grid (input power) which results in spikes in the input current.

The DB-DTFC torque response for Fig. 10 can be analyzed further in Fig. 11. The torque command with the estimated torque is clearly demonstrated. The battery current increases to 3 A immediately responding to the torque.

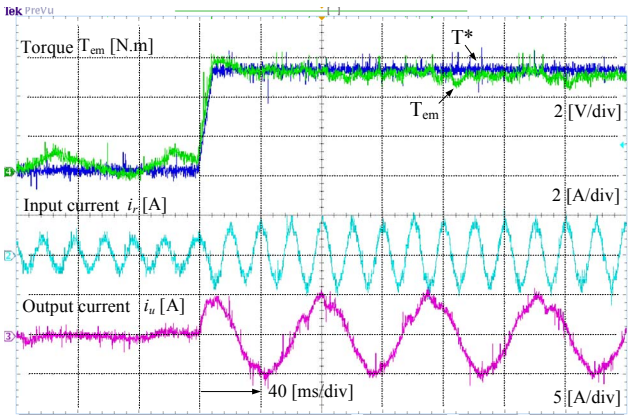

Fig.9. Experimental result obtained from IMC only showing fast torque response tracking the torque command

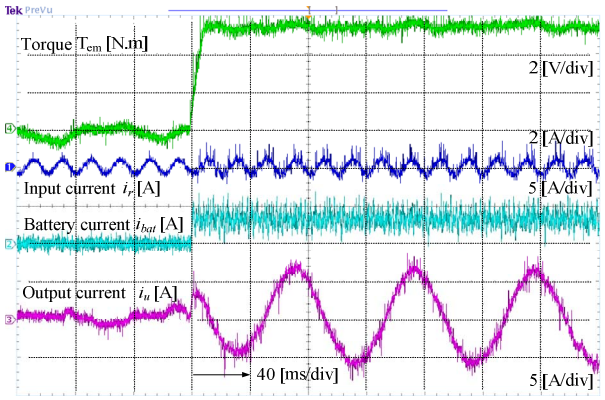

Fig. 10 Experimental result obtained from the proposed circuit structure showing the battery current increasing immediately in response to the output current while the input current is shown to remain unchanged.

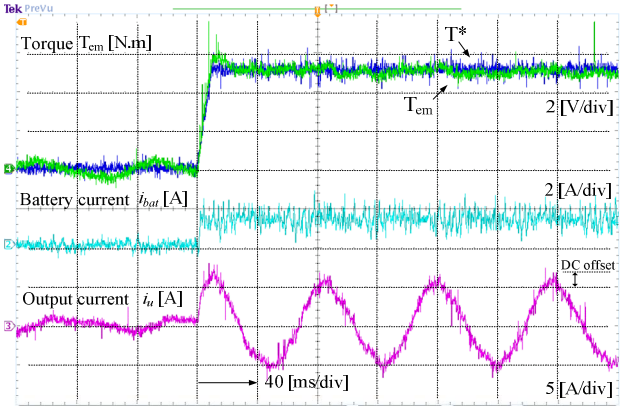

Fig. 11 Experimental result obtained from the proposed circuit structure showing that battery power is utilized instead of input power and that the torque response is fast to achieve the torque command.

Similarly, dynamic fast torque response can be produced to reach the desired value (5 Nm). The DC offset on the output current can be noticed in the result. This result demonstrates that the estimated torque as well as the torque response is not affected by the DC offset component.

Fig. 12 compares the torque ripple by using FFT analysis on the estimated steady state torque (at 5 Nm). Fig. 12(a) shows the condition of Fig. 9 and Fig. 12(b) shows the condition of Fig. 11. Fig. 12 (b) uses a smaller scaling on the frequency so that it can clearly indicate that the torque ripple does not increase due to the RFBC connection. That is, the existence of battery current in the motor current does not produce nor increase the torque ripple. Comparing Figs. 12 (a) and (b), though the modulation scheme for inverter is applied with the variable frequency carrier comparison PWM, the torque ripple can remain low.

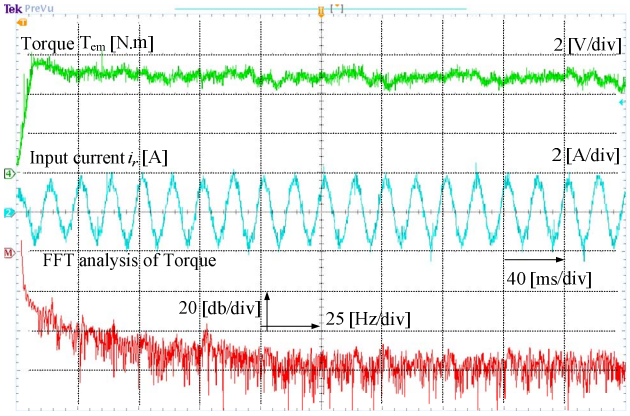

Fig.12(a) Analysis of harmonic components on the estimated steady state torque. Experiment condition is consistent to Fig. 9. The graphical division for FFT is 20 db/div and 25 Hz/div.

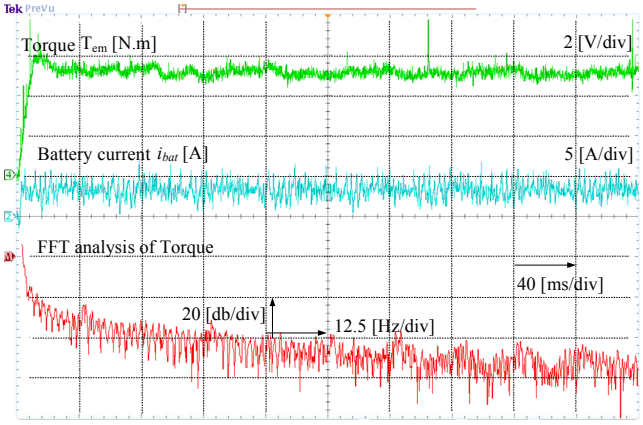

Fig. 12(b) Analysis of harmonic components on the estimated steady state torque. Experiment condition is consistent to Fig. 11. The graphical division for FFT is 20 db/div and 12.5 Hz/div

VI. Conclusions

This paper presents the performance of DB-DTFC under two different converters, a standard fixed switching frequency inverter and a proposed variable switching frequency IMC/RFBC circuit. The first section evaluated the voltage utilization (Volt-sec) produced from DB-DTFC by using two modulation schemes, carrier comparison PWM and SVM, in a fixed switching frequency inverter. From the experimental implementation, the results show that the SVM was able to deliver 1.5 % more voltage magnitude than the carrier comparison PWM.

The second section documented the torque response and ripple behavior obtained when DB-DTFC was implemented using the proposed IMC/RFBC circuit. The results effectively show that DB-DTFC is capable of delivering fast transient torque response when battery power is used from the RFBC connection. Furthermore, the torque ripple was shown to be low even when the inverter stage of the IMC is implemented with a variable frequency carrier comparison PWM.

References

[1] Kolar, J.W., Friedli, T., Rodriguez, J. and Wheeler, P.W. "Review of three-phase AC-AC converter topologies", *IEEE Trans. on Industrial Electronics*, Vol. 58, Issue. 11, pp. 4988-5006, Nov. 2011.

[2] Rixin Lai, Fei Wang, Burgos, R., Yunqing Pei, Boroyevich, D., Bigsen Wang, Lipo, T.A., Immanuel, V.D., and Karimi, K.J. "A systematic topology evaluation methodology for high density three-phase PWM AC-AC converters", *IEEE Trans. on Power Electronics*, Vol. 23, Issue. 6, pp. 2665-2680, Nov. 2008.

[3] Kolar, J.W., Schafmeister, F., Round, S.D and Ertl, H. "Novel three-phase AC-AC sparse matrix converters", *IEEE Trans. on Power Electronics*, Vol. 22, Issue. 5, pp. 1649-1661, Sept. 2007.

[4] Jussila, M. and Tuusa, H. "Comparison of simple control strategies of space vector modulated indirect matrix converter under distorted supply voltage", *IEEE Trans. on Power Electronics*, Vol. 22, Issue. 1, pp. 139-1448, Jan. 2007.

[5] Goh Teck Chiang and Jun-ichi Itoh: "DC/DC Boost Converter Functionality in a Three-phase Indirect Matrix Converter", *IEEE Transactions on Power Electronics*, Vol. 26, Issue. 5, October 2011.

[6] Goh Teck Chiang and Jun-ichi Itoh: "Comparison of two overmodulation strategies in an Indirect Matrix Converter", *IEEE Transactions on Industrial Electronics*, 2012 [available online]

[7] M. F. Rahman, L. Zhong, and K. W. Lim, "A direct torque-controlled interior permanent magnet synchronous motor drive incorporating field weakening", *IEEE Trans Industry Applications,* Vol. 34, pp. 1246-1253, Nov. 1998.

[8] Inoue, Y., Morimoto, S. and Sanada, M. "Examination and Linearization of Torque Control System for Direct Torque Controlled IPMSM", *IEEE Trans Industry Applications,* Vol. 46, pp. 159-166, Jan. 2010.

[9] West, N.T and Lorenz, R.D. "Digital Implementation of Stator and Rotor Flux Linkage Observers and a Stator-Current Observer for Deadbeat Direct Torque Control of Induction Machines", *IEEE Trans Industry Applications,* Vol. 45, pp. 729-736, March 2009.

[10] Jae Suk Lee, Chan-Hee Choi, Jul-Ki Seok and Lorenz, R.D. "Deadbeat-Direct Torque and Flux Control of Interior Permanent Magnet Synchrnous Machines with Discrete Time Stator Current and Stator Flux Linkage Observer", *IEEE Trans Industry Applications,* Vol. 47, pp. 1749-1758, May 2011.

[11] Yongchang Zhang, "A Novel Duty Cycle Control Strategy to Reduce Both Torque and Flux Ripples for DTC of Permanent Magnet Synchronous Motor Drives with Switching Frequency Reduction", *IEEE Transactions on Power Electronics*, Vol. 26, Issue. 10, October 2011.